ChemComm

Cite this: *Chem. Commun.*, 2012, **48**, 5172–5174

www.rsc.org/chemcomm

COMMUNICATION

Highly enantioselective asymmetric hydrogenation of (*E*)-β,β-disubstituted α,β-unsaturated Weinreb amides catalyzed by Ir(I) complexes of SpinPhox ligands†

Jian Shang, Zhaobin Han, Yang Li, Zheng Wang and Kuiling Ding*

Received 4th February 2012, Accepted 2nd April 2012
DOI: 10.1039/c2cc30812f

The Ir(I) complexes of chiral spiro phosphino–oxazoline ligands (SpinPhox) have demonstrated good to excellent enantioselectivity in the asymmetric hydrogenation (AH) of a variety of (*E*)-β,β-disubstituted α,β-unsaturated *N*-methoxy-*N*-methylamides, affording the corresponding optically active Weinreb amides with up to 97% ee.

N-Methoxy-*N*-methylamides, well-known as Weinreb amides,[1] have been established as an important class of acylating agents with numerous synthetic utilities.[2] Given the wide utilities of optically active Weinreb amides as a stable chiral acylating agent in asymmetric synthesis, development of novel and efficient methodologies for their synthesis would be highly desirable. Among the rare examples, Hayashi *et al.* reported in 2005 a Rh-catalyzed highly enantioselective asymmetric 1,4-addition of arylboronic acids to α,β-unsaturated Weinreb amides.[3] Very recently, Takacs *et al.* demonstrated that β,γ-unsaturated Weinreb amides are amenable to Rh-catalyzed asymmetric hydroboration, to afford chiral organoboronates that can be easily transformed into chiral ketones or aldehydes.[4] Clarke *et al.* reported an Rh/diphosphine catalyzed highly regioselective asymmetric hydroformylation of acrylic Weinreb amide to give the enantio-enriched aldehyde.[5] We envisioned that transition metal catalyzed AH[6] of the readily accessible prochiral unsaturated *N*-methoxy-*N*-methylamides would be an efficient and atom-economical route to optically active Weinreb amides. While some excellent Ir-based catalytic systems have been reported for AH of C=C double bonds in α,β-unsaturated carbonyl compounds in general,[7] examples that are especially effective for the AH of α,β-unsaturated amides are relatively rare.[8] In particular, to the best of our knowledge, there has been no systematic study on the catalytic AH of unsaturated Weinreb amides so far.[9] Herein, we present the iridium-catalyzed AH[10] of (*E*)-β,β-disubstituted α,β-unsaturated Weinreb amides with iridium(I) complexes **3** bearing a spiro P^N ligand[11,12] (SpinPhox)[13] as the catalysts.

State Key Laboratory of Organometallic Chemistry, Shanghai Institute of Organic Chemistry, Chinese Academy of Sciences, 345 Lingling Road, Shanghai, 200032, P.R. China. E-mail: kding@mail.sioc.ac.cn; Fax: +86 21 64166128

† Electronic supplementary information (ESI) available: Experimental details and characterization data for all new compounds. CCDC 822915 ((*R*,*S*)-**3a**) and 865426 ((*S*,*S*)-**3c**). For ESI and crystallographic data in CIF or other electronic format see DOI: 10.1039/c2cc30812f

The α,β-unsaturated Weinreb amide substrates **1a–r** were readily synthesized in good to high yields by following a literature method (see ESI†).[14] The chiral iridium complexes (*R*,*S*)-**3a–e** and (*S*,*S*)-**3b–e** were synthesized according to our previously published procedure.[13a] To examine the feasibility of the catalysis, initial investigations were performed with **1a** as the model substrate and (*R*,*S*)-**3a** as the catalyst. As shown in Table 1, the solvent effect is dramatic for this reaction (entries 1–7), and dichloromethane was found to be the superior solvent (92% conversion, 89% ee). Lowering the initial hydrogen pressure from 50 to 20 atm resulted in a marked decline in the substrate conversion (92 *vs.* 66%, entries 1 and 8), albeit the effect on the enantioselectivity is only marginal (89 *vs.* 87% ee).

Table 1 Screening of reaction conditions for (*R*,*S*)-**3a**-catalyzed AH of α,β-unsaturated Weinreb amide **1a**[a]

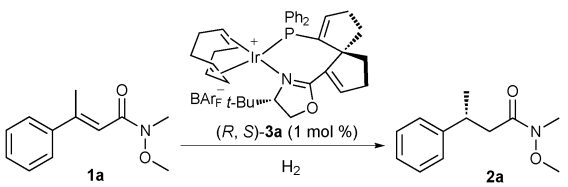

Entry	Solvent	$P(H_2)$/atm	T/°C	Conv.[b] (%)	ee[c] (%)
1	CH_2Cl_2	50	25	92	89
2	DCE	50	25	74	89
3	$CHCl_3$	50	25	57	89
4	$PhCH_3$	50	25	26	77
5	Et_2O	50	25	14	6
6	EtOAc	50	25	38	66
7	MeOH	50	25	33	20
8	CH_2Cl_2	20	25	66	87
9	CH_2Cl_2	20	40	32	81
10	CH_2Cl_2	50	40	70	89
11	CH_2Cl_2	50	50	77	88
12[d]	CH_2Cl_2	20	25	5	N.D.
13[e]	CH_2Cl_2	50	25	>99	89

[a] Unless otherwise specified, all reactions were carried out with 0.1 mmol of the substrate ([**1a**] = 0.1 M) in 1.0 ml of the solvent for 24 h, in the presence of 0.001 mmol (1 mol%) of the Ir catalyst (*R*,*S*)-**3a**. [b] Determined by ^{1}H NMR analysis. [c] Determined by HPLC on a chiral AD-H column. In all cases, the absolute configuration of **2a** was determined to be (*R*) by comparison of the corresponding specific rotations with the literature value. [d] Ir(I)/(*S*)-*t*BuPHOX was used as the catalyst. N.D. = not determined. [e] [(*R*, *S*)-**3a**] = 2 mM (2 mol%).

Table 2 Catalyst optimization for the SpinPhox–Ir-catalyzed AH of **1a**[a]

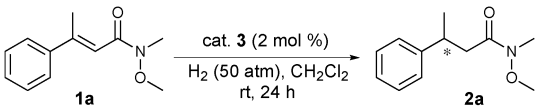

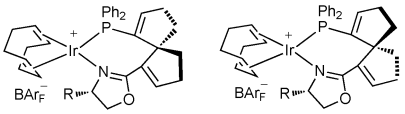

(*R*, *S*)-**3a-e**

(*R*, *S*)-**3a** R = *t*-Bu
(*R*, *S*)-**3b** R = Bn
(*R*, *S*)-**3c** R = Ph
(*R*, *S*)-**3d** R = *i*-Bu
(*R*, *S*)-**3e** R = *i*-Pr

(*S*, *S*)-**3b-e**

(*S*, *S*)-**3b** R = Bn
(*S*, *S*)-**3c** R = Ph
(*S*, *S*)-**3d** R = *i*-Bu
(*S*, *S*)-**3e** R = *i*-Pr

Entry	Catalyst	Conv.[b] (%)	ee[c] (%)
1	(*R*,*S*)-**3a**	>99	89 (*R*)
2	(*R*,*S*)-**3b**	>99	95 (*R*)
3	(*R*,*S*)-**3c**	36	79 (*R*)
4	(*R*,*S*)-**3d**	29	82 (*R*)
5	(*R*,*S*)-**3e**	70	77 (*R*)
6	(*S*,*S*)-**3b**	18	61 (*S*)
7	(*S*,*S*)-**3c**	>99	84 (*S*)
8	(*S*,*S*)-**3d**	6	50 (*S*)
9	(*S*,*S*)-**3e**	34	45 (*S*)
10[d]	(*R*,*S*)-**3b**	88	94 (*R*)
11[e]	(*R*,*S*)-**3b**	98	94 (*R*)

[a] Reaction conditions: [**1a**] = 0.1 M, [**3**] = 2 mM (2 mol%), T = 25 °C, $P(H_2)$ = 50 atm, t = 24 h, dichloromethane solvent. [b] Determined by ^{1}H NMR analysis. [c] Determined by HPLC (chiral AD-H column). The absolute configuration was assigned by comparison of the specific rotation with the literature value. [d] t = 12 h. [e] T = 0 °C.

Elevation of the reaction temperature from rt to 50 °C also exhibited a minor effect on the enantioselectivity, however, the conversion of **1a** decreased considerably presumably as a result of catalyst decomposition (entries 1 *vs.* 10 and 11, entries 8 *vs.* 9). The use of an Ir(I) complex of an analogous *t*BuPHOX ligand[11a] afforded only 5% conversion of **1a** under the identical experimental conditions (entry 12). Finally, the full conversion of **1a** in 24 h was realised under 50 atm of H_2 in CH_2Cl_2 by increasing the catalyst (*R*,*S*)-**3a** loading from 1 to 2 mol% (entry 13).

To further improve the enantioselectivity of the catalysis, a range of (*R*,*S*)-**3** or (*S*,*S*)-**3** catalysts were screened in the AH of **1a** under the above-mentioned optimized reaction conditions. As shown in Table 2, the chirality at the spiro backbone of the ligands obviously plays a key role in determining the stereochemical outcome of the asymmetric induction, as the (*R*,*S*)- and (*S*,*S*)-catalysts **3** always afforded the hydrogenation product **2a** with opposite absolute configurations (entries 1–5 *vs.* 6–9). The (*R*,*S*)-**3b**, **3d**, and **3e** generally demonstrated a higher conversion and ee value than their corresponding (*S*,*S*)-analogues (entries 2, 4 and 5 *vs.* 6, 8 and 9, respectively), even though irregularities do exist for the catalysis by (*R*,*S*)- or (*S*,*S*)-**3c** (entries 3 *vs.* 7). This observation suggests that the (*R*,*S*)-**3** tend to be the chirality-matched catalysts for enantioselectivity control. Among the Ir complexes (*R*,*S*)-**3a–e** bearing various oxazolinyl substituents, (*R*,*S*)-**3b** turned out to be optimal in terms of both reactivity and enantioselectivity (>99% conversion, 95% ee, entry 2).

With these results in hand, we proceeded to further extend the substrate scope by examining AH of (*E*)-β,β-disubstituted

Table 3 (*R*,*S*)-**3b** catalyzed AH of (*E*)-β,β-disubstituted α,β-unsaturated Weinreb amides[a]

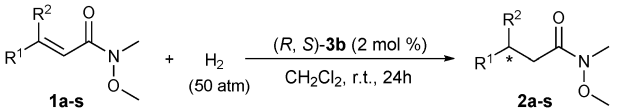

Entry	Substrate	R^1	R^2	Conv.[b] (%)	ee[c] (%)
1	**1a**	C_6H_5	Me	>99	95 (*R*)
2	**1b**	4-MeC_6H_4	Me	>99	97 (*R*)
3	**1c**	4-MeOC_6H_4	Me	>99	96 (*R*)
4	**1d**	2,4-$(MeO)_2C_6H_3$	Me	>99	83 (+)
5	**1e**	4-*i*-BuC_6H_4	Me	>99	96 (+)
6	**1f**	4-FC_6H_4	Me	>99	96 (+)
7	**1g**	4-ClC_6H_4	Me	>99	94 (+)
8	**1h**	4-IC_6H_4	Me	>99	94 (+)
9	**1i**	4-F_3CC_6H_4	Me	>99	92 (+)
10	**1j**	3-MeOC_6H_4	Me	>99	95 (+)
11	**1k**	3-ClC_6H_4	Me	>99	95 (+)
12	**1l**	2-MeC_6H_4	Me	>99	82 (+)
13	**1m**	Naphthalen-2-yl	Me	>99	95 (*R*)
14	**1n**	Naphthalen-1-yl	Me	>99	79 (+)
15	**1o**	Benzyl	Me	>99	91 (+)
16	**1p**	*t*-Bu	Me	12	N.D.[d]
17	**1q**	C_6H_5	Et	>99	96 (+)
18	**1r**	C_6H_5	*i*-Pr	94	90
19[e]	**1s**	*n*-Bu	Me	>99	65 (+)
20[f]	**1a**	C_6H_5	Me	>99	97

[a] For reaction conditions, see footnote *a* in Table 2. [b] Determined by ^{1}H NMR analysis. [c] Determined by HPLC on a chiral AD-H column. The absolute configurations were assigned by comparison of the corresponding specific rotations with the literature values. [d] Not determined. [e] The catalyst loading is 6 mol%. [f] The quantity of **1a** in this case is 1.0 mmol.

α,β-unsaturated Weinreb amides **1a–s**. As shown in Table 3, for the reactions of substrates with a Me group at their β-position (**1a–o**), quantitative conversions were generally attained in 24 h, and enantioselectivities were good to excellent, ranging from 79 to 97% ee (entries 1–15). Among these substrates, reactions involving those with a *para*- or *meta*-substituted β-phenyl ring (**1a–c** and **1e–k**) afforded uniformly high ee values (92–97%, entries 1–3 and 5–11), irrespective of the electron-donating or electron-withdrawing nature of the substituent. In contrast, the enantioselectivities were slightly lower for reactions involving **1d** and **1l**, both having a sterically somewhat more demanding *ortho*-substituent on their β-phenyl rings. These observations suggest that the steric properties of the β-substituent seem to play a more substantial role than the electronic ones in determining the enantioselectivity, and the steric congestion of the β-substituent should have a negative impact on the catalysis. This was also confirmed by the performance of reactions involving **1m** and **1n** with a β-2- or β-1-naphthyl substituent (95 *vs.* 79% ee, entries 13 and 14), which can formally be viewed as 3,4- or 2,4-disubstituted phenyl rings, respectively. Furthermore, the reactions involving (*E*)-β,β-dialkyl substituted amides **1o**, **1p**, and **1s** are also consistent with this generalized trend. While AH of **1o** afforded the corresponding product in full conversion with 91% ee (entry15), the reaction with **1p** that bears a bulky β-*t*-Bu group proceeded much more sluggishly to afford only a poor conversion (12%, entry 16), and the reaction with **1s** needs higher catalyst loading (6 mol%) for full conversion (entry 19). In addition, AH of substrate **1q** gave a result comparable to that of its homologue **1a** (entries 17 *vs.* 1),

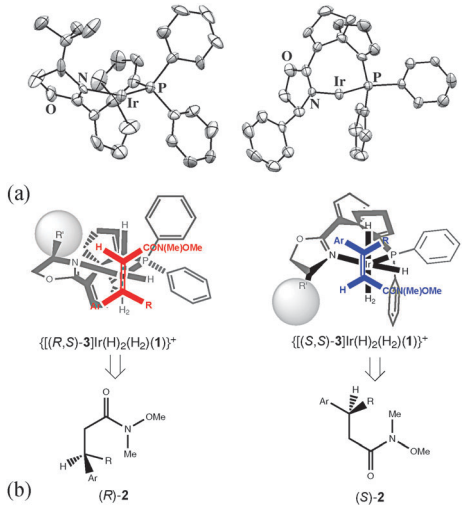

Fig. 1 (a) X-Ray structures of (*R*,*S*)-**3a** (left) and (*S*,*S*)-**3c** (right), H atoms, BAr_F^- anion, and 1,5-cyclooctadiene are omitted for clarity. (b) Schematic model for enantioselection of (*R*,*S*)- and (*S*,*S*)-**3**.

whereas the reaction with sterically somewhat more crowded **1r** resulted in incomplete conversion (94%) and a slightly declined ee value (90%, entry 18). Finally, the procedure can be scaled up to 1.0 mmol of the substrate, with even a slightly higher ee value being obtained in the case of **1a** (entry 20 *vs.* 1).

The structures of catalyst precursors (*R*,*S*)-**3a** and (*S*,*S*)-**3c** have been determined by single crystal X-ray diffraction (Fig. 1a, see ESI† for details).[15] Inspired by the elegant DFT study reported recently by Andersson *et al.*[16] on the mechanism of Ir/P^N catalyzed hydrogenation of unfunctionalized olefins as well as the structures of (*R*,*S*)-**3a** and (*S*,*S*)-**3c** (Fig. 1a), we tentatively propose a schematic model to account for the stereoselection in the (*R*,*S*)- or (*S*,*S*)-**3** catalyzed hydrogenation of unsaturated amides **1**, a class of trisubstituted olefins. As shown in Fig. 1b, the bulky oxazolyl substituent is forced to situate either above or below the equatorial plane defined by N–Ir–P of the catalytic intermediates $\{[(R,S)\text{-}\mathbf{3}]Ir(H)_2(H_2)(\mathbf{1})\}^+$ or $\{[(S,S)\text{-}\mathbf{3}]Ir(H)_2(H_2)(\mathbf{1})\}^+$, respectively, as a result of the constraints of the rigid spiro ligand backbone. The unsaturated amide is coordinated *trans* to the phosphorous moiety, and oriented with the smallest substituent (H atom) pointing towards the oxazoline fragment. The sense of enantioselection predicted on the basis of this model can rationalize the opposite asymmetric inductions in AH of **1a** using (*R*,*S*)- or (*S*,*S*)-**3** catalysts (Table 2).

In summary, catalytic AH of α,β-unsaturated Weinreb amides using chiral Ir catalysts **3** has provided an efficient and clean route to enantio-enriched Weinreb amides. Full conversions and excellent ee values (up to 97%) can be obtained under the optimized conditions, and the sterically less bulky substituents at the β-position seem to be more amenable to the present catalytic protocol. Given the easy access to various unsaturated Weinreb amide substrates, such a catalytic AH methodology is expected to find broad applications in the preparation of optically active Weinreb amides.

Financial support from NSFC (No. 21172237, 21121062, 21032007), the Major Basic Research Development Program of China (Grant No. 2010CB833300), and the Chinese Academy of Sciences is gratefully acknowledged.

Notes and references

1 S. Nahm and S. M. Weinreb, *Tetrahedron Lett.*, 1981, **22**, 3815.
2 For reviews, see: (*a*) M. P. Sibi, *Org. Prep. Proced. Int.*, 1993, **25**, 15; (*b*) M. Mentzel and H. M. R. Hoffmann, *J. Prakt. Chem.*, 1997, **339**, 517; (*c*) J. Singh, N. Satyamurthi and I. S. Aidhen, *J. Prakt. Chem.*, 2000, **342**, 340; (*d*) S. Balasubramaniam and I. S. Aidhen, *Synthesis*, 2008, 3707.
3 R. Shintani, T. Kimura and T. Hayashi, *Chem. Commun.*, 2005, 3213.
4 S. M. Smith, M. Uteuliyev and J. M. Takacs, *Chem. Commun.*, 2011, **47**, 7812.
5 G. M. Noonan, D. Newton, C. J. Cobley, A. Suárez, A. Pizzano and M. L. Clarke, *Adv. Synth. Catal.*, 2010, **352**, 1047.
6 For reviews, see: (*a*) *Handbook of Homogeneous Hydrogenation*, ed. J. G. de Vries and C. J. Elsevier, Wiley VCH, Weinheim, 2007; (*b*) G. Shang, W. Li and X. Zhang, in *Catalytic Asymmetric Synthesis*, ed. I. Ojima, Wiley, Hoboken, 3rd edn, 2010, pp. 343–436.
7 For examples, see: (*a*) S.-M. Lu and C. Bolm, *Angew. Chem., Int. Ed.*, 2008, **47**, 8920; (*b*) W. Lu, Y. Chen and X. Hou, *Angew. Chem., Int. Ed.*, 2008, **47**, 10133; (*c*) S. M. Lu and C. Bolm, *Chem.–Eur. J.*, 2008, **14**, 7513; (*d*) F. T. Tian, D. M. Yao, Y. Y. Liu, F. Xie and W. B. Zhang, *Adv. Synth. Catal.*, 2010, **352**, 1841; (*e*) D. Liu, W. J. Tang and X. Zhang, *Org. Lett.*, 2004, **6**, 513; (*f*) J. G. Zhou, J. W. Ogle, Y. B. Fan, V. Banphavichit, Y. Zhu and K. Burgess, *Chem.–Eur. J.*, 2007, **13**, 7162; (*g*) S. Li, S. F. Zhu, C. M. Zhang, S. Song and Q. L. Zhou, *J. Am. Chem. Soc.*, 2008, **130**, 8584; (*h*) S. Li, S. F. Zhu, J. H. Xie, S. Song, C. M. Zhang and Q. L. Zhou, *J. Am. Chem. Soc.*, 2010, **132**, 1172; (*i*) D. H. Woodmansee, M. A. Muller, M. Neuburger and A. Pfaltz, *Chem. Sci.*, 2010, **1**, 72; (*j*) D. Rageot, D. H. Woodmansee, B. Pugin and A. Pfaltz, *Angew. Chem., Int. Ed.*, 2011, **50**, 9598.
8 W.-J. Lu and X.-L. Hou, *Adv. Synth. Catal.*, 2009, **351**, 1224 and the references therein.
9 Burgess reported an example of chiral NHC–Ir catalyzed AH of a Weinreb amide derivative with a moderate ee value (46%), see ref. 7*f*.
10 For reviews, see: (*a*) S. J. Roseblade and A. Pfaltz, *Acc. Chem. Res.*, 2007, **40**, 1402; (*b*) X. Cui and K. Burgess, *Chem. Rev.*, 2005, **105**, 3272; (*c*) K. Källström, I. Munslow and P. G. Andersson, *Chem.–Eur. J.*, 2006, **12**, 3194; (*d*) Y.-G. Zhou, *Acc. Chem. Res.*, 2007, **40**, 1357; (*e*) D. H. Woodmansee and A. Pfaltz, *Chem. Commun.*, 2011, **47**, 7912.
11 For reviews, see: (*a*) G. Helmchen and A. Pfaltz, *Acc. Chem. Res.*, 2000, **33**, 336; (*b*) H. A. McManus and P. J. Guiry, *Chem. Rev.*, 2004, **104**, 4151; (*c*) I. D. Kostas, *Curr. Org. Synth.*, 2008, **5**, 227.
12 The spirobackbone based chiral ligands in asymmetric catalysis, see: (*a*) *Privileged Chiral Ligands and Catalysts*, ed. Q.-L. Zhou, Wiley-VCH, Weinheim, 2011; (*b*) A. S. C. Chan, W. Hu, C.-C. Pai, C.-P. Lau, Y. Jiang, A. Mi, M. Yan, J. Sun, R. Lou and J. Deng, *J. Am. Chem. Soc.*, 1997, **119**, 9570; (*c*) J.-H. Xie and Q.-L. Zhou, *Acc. Chem. Res.*, 2008, **41**, 581; (*d*) K. Ding, Z. Han and Z. Wang, *Chem.–Asian J.*, 2009, **4**, 32; (*e*) G. B. Bajracharya, M. A. Arai, P. S. Koranne, T. Suzuki, S. Takizawa and H. Sasai, *Bull. Chem. Soc. Jpn.*, 2009, **82**, 285.
13 (*a*) Z. Han, Z. Wang, X. Zhang and K. Ding, *Angew. Chem., Int. Ed.*, 2009, **48**, 5345; (*b*) Y. Zhang, Z. Han, F. Li, K. Ding and A. Zhang, *Chem. Commun.*, 2010, **46**, 156; (*c*) X. Wang, Z. Han, Z. Wang and K. Ding, *Angew. Chem., Int. Ed.*, 2012, **51**, 936.
14 W. S. Wadsworth, *Organic Reactions*, J. R. Wiley and Sons, New York, 1977, vol. 25, pp. 73–253.
15 CCDC 822915 ((*R*,*S*)-**3a**) and CCDC 865426 ((*S*,*S*)-**3c**) contain the supplementary crystallographic data for this paper.
16 T. L. Church, T. Rasmussen and P. G. Andersson, *Organometallics*, 2010, **29**, 6769 and the references cited therein.

